# Delocalization effects and charge reorganizations induced by repulsive interactions in strongly disordered chains

D. Weinmann[1,2], P. Schmitteckert[1,3], R.A. Jalabert[1,a], and J.-L. Pichard[4]

[1] Institut de Physique et Chimie des Matériaux de Strasbourg[b], 23 rue du Loess, 67037 Strasbourg Cedex, France
[2] Institut für Physik, Universität Augsburg, 86135 Augsburg, Germany
[3] Fridolinstr. 19, 68753 Waghäusel, Germany
[4] CEA, Service de Physique de l'État Condensé, Centre d'Études de Saclay, 91191 Gif-sur-Yvette Cedex, France

**Abstract.** We study the delocalization effect of a short-range repulsive interaction on the ground state of a finite density of spinless fermions in strongly disordered one dimensional lattices. The density matrix renormalization group method is used to explore the charge density and the sensitivity of the ground state energy with respect to the boundary condition (the persistent current) for a wide range of parameters (carrier density, interaction and disorder). Analytical approaches are developed and allow to understand some mechanisms and limiting conditions. For weak interaction strength, one has a Fermi glass of Anderson localized states, while in the opposite limit of strong interaction, one has a correlated array of charges (Mott insulator). In the two cases, the system is strongly insulating and the ground state energy is essentially invariant under a twist of the boundary conditions. Reducing the interaction strength from large to intermediate values, the quantum melting of the solid array gives rise to a more homogeneous distribution of charges, and the ground state energy changes when the boundary conditions are twisted. In individual chains, this melting occurs by abrupt steps located at sample-dependent values of the interaction where an (avoided) level crossing between the ground state and the first excitation can be observed. Important charge reorganizations take place at the avoided crossings and the persistent currents are strongly enhanced around the corresponding interaction value. These large delocalization effects become smeared and reduced after ensemble averaging. They mainly characterize half filling and strong disorder, but they persist away of this optimal condition.

**PACS.** 72.15.-v Electronic conduction in metals and alloys – 73.20.Dx Electron states in low-dimensional structures (superlattices, quantum well structures and multilayers) – 72.10.Bg General formulation of transport theory – 05.60.Gg Quantum transport

## 1 Introduction

One of the beauties of Condensed Matter Physics is the possibility of understanding a variety of phenomena within a (weakly interacting) quasi-particle approach, despite the always present strong Coulomb interaction between electrons. As it has been understood from the early days [1], the applicability of one-particle approaches can be traced to the Pauli exclusion principle, and in first approximation the interactions simply account for a renormalization of single-particle quantities (like the effective mass or the mean field potential felt by individual electrons).

This traditional view is challenged when studying artificially confined mesoscopic systems or very dilute low-dimensional electron gases. Mesoscopic phenomena have their origin in the coherence of electronic wave functions across a small sample. The reduced dimensions are expected to render electronic correlations more important than in the bulk. Going to lower dimensions and/or very dilute limits results in a poorer screening of the electron-electron interaction, enhancing the role of Coulomb repulsions. When the disorder is strong, Anderson localization becomes also detrimental to screening, thereby further magnifying the role of interactions.

The above considerations are closely related to three experimental findings which have recently dominated the attention in Mesoscopic Physics. Firstly, the large values of the persistent current measured in metallic mesoscopic rings [2–4] cannot be accounted by the theoretical predictions based on the single electron picture [5], nor by perturbative approaches taking into account (to infinite order) the effect of electron-electron interactions [6,7]. Secondly, the discovery of a metallic behavior in two-dimensional gases of electrons (Si-MOSFET [8]) or holes (GaAs heterostructures [9] and SiGe quantum wells [10]) is at odds with the conclusions of non-interacting theories that predict an insulating behavior for any value of the

disorder strength [11]. For a recent review on the metal-insulator transition in 2D electron and hole gases see reference [12]. The metallic behavior is observed in a parameter region of the system which is believed to be limited by its crystallization threshold [13,14]. Finally, the conventional view of an infinite zero-temperature quasiparticle lifetime at the Fermi energy has been questioned by the interpretation of measurements yielding a saturation of the electronic decoherence rate with decreasing temperature [15]. While a complete understanding of these findings is still missing, it is widely accepted that they are influenced in a non-trivial way by large interaction effects. Recent theoretical attempts suggest a possible relation between these different phenomena [16–18].

In this work we study the persistent current and the localization within a model of spinless electrons on a disordered one-dimensional (1D) ring with nearest-neighbor interactions. Clearly, we do not aim to describe the metallic quasi-one dimensional rings of references [2–4] nor the two-dimensional electron gas where the metal-insulator transition has been observed. However, the interplay between localization and interaction can be readily studied in this simple model. The interest on disordered one-dimensional interacting models of fermions (with and without spin) can also be assessed from the large variety of analytical [19–24] and numerical [25–32] techniques that have been applied to them.

In the absence of interactions, a 1D disordered system is an Anderson insulator, with the electron wavefunctions localized on the scale of the one-particle localization length $\xi_1$. The dependence of the conductance on the size $M$ of the system is given by an exponential decrease, the characteristic length scale being determined by $\xi_1$. If the system is closed into a ring threaded by a magnetic flux, its orbital response (the persistent current) also scales exponentially with $M/\xi_1$ [33].

In rotational invariant continuum systems the persistent current does not depend on any kind of interactions [22,24]. This is directly connected to the fact that the Drude weight (to be defined in the sequel) is not affected by electron-electron interactions in Galilean invariant systems [34]. When the rotational invariance is broken by a lattice or by the presence of disorder, interactions can modify the value of the persistent current [30].

The problem of spinless fermions in a disorder-free chain with nearest-neighbor interactions is exactly solvable [19]. In particular, at half filling we have a Mott insulator with a finite gap and a charge density wave concentrated on alternating sites of the lattice. Attractive interactions favor an inhomogeneous density (clustering). Repulsive interactions favor a homogeneous density (charge density wave or Mott insulator). Disorder tends to distort those arrangements by favoring the occupancy of the low potential sites. In the intermediate regime between the Anderson and Mott insulators, disorder, interaction and kinetic energy are relevant. The competition between disorder and interactions that we study throughout our work exhibits then a non-trivial character.

The localized character of an electron system determines the behavior of the conductance, which is a transport property, as well as the persistent current, which is a thermodynamic property. As first shown by Kohn [35], in the zero temperature limit, both properties can be related. We recall the basic ingredients of such a relationship [22, 35,36] for the particular case of the insulating regime.

The linear response of the electronic system to a spatially uniform, time-dependent electric field is the frequency-dependent conductivity

$$\sigma(\omega) = \sigma_1(\omega) + i\sigma_2(\omega). \tag{1}$$

A 1D ring containing $M$ sites, threaded by a magnetic flux $\Phi$ has a flux-dependent many-particle ground state energy $E(\Phi)$. We choose units such that $\hbar = e^2 = c = a = 1$ ($a$ is the lattice constant), and $\Phi = 2\pi$ corresponds to one flux quantum threading the ring. Kohn showed that the second derivative of $E(\Phi)$ (the charge stiffness or Kohn curvature)

$$D_c = M \left( \frac{d^2 E(\Phi)}{d\Phi^2} \right) \Bigg|_{\Phi=0} \tag{2}$$

is related to the imaginary part $\sigma_2(\omega)$ of the conductivity through

$$D_c = \lim_{\omega \to 0} \omega \, \sigma_2(\omega). \tag{3}$$

Using the Kramers-Kronig relations between the real and the imaginary part of the conductivity (see, *e.g.* [22]), it is found that $D_c$ also gives the weight of the zero-frequency peak in the real part of the conductivity

$$\sigma_1(\omega) = \pi D_c \delta(\omega) + \sigma_1^{reg}(\omega). \tag{4}$$

Therefore, $D_c$ is sometimes called the Drude weight. This establishes a link between transport properties and persistent currents.

In the insulating regime the amplitude of the flux-dependent oscillation of the ground state energy is typically much smaller than the energy gap between the many-body ground state and the first excited state. Therefore, it is easy to see (*i.e.* Sect. 4) that a perturbation theory in the hopping matrix elements across the boundary is enough to describe the flux dependence of the ground state energy, which yields

$$E(\Phi) = E(0) - \frac{\Delta E}{2}(1 - \cos\Phi). \tag{5}$$

Here $\Delta E = E(0) - E(\pi)$ can also be interpreted as the difference of ground state energy between periodic ($\Phi = 0$) and anti-periodic ($\Phi = \pi$) boundary conditions, since a magnetic flux through the ring is equivalent to introducing a change of the boundary conditions. The sign of $\Delta E$ depends only on the parity of the number of particles $N$ ($\Delta E < 0$ for odd $N$ and $\Delta E > 0$ for even $N$) [37,38].

The simple $\Phi$-dependence of the ground state energy in equation (5) allows to relate $\Delta E$ to the persistent current

$$J(\Phi) = -\frac{dE(\Phi)}{d\Phi} = \frac{\Delta E}{2}\sin\Phi, \tag{6}$$

and the Drude weight

$$D_{\rm c} = -\frac{M}{2}\Delta E. \tag{7}$$

In this paper we will work extensively with the *phase sensitivity*

$$D = (-1)^N \frac{M}{2}\Delta E, \tag{8}$$

that for a *strongly disordered one-dimensional ring* is simply given by the absolute value of the Drude weight and, at the same time, determines the magnitude of the persistent current.

The possibility of a negative charge stiffness (or $D_{\rm c}$) arising for spinless fermions and Hubbard rings [39,40] indicates that the orbital response may be paramagnetic. This is a peculiar behavior since $D_{\rm c}$ is believed to determine the zero-frequency behavior of $\sigma_1$.

The previous numerical work on interacting disordered rings has necessarily been restricted to finite samples [26,27] or it has relied on strong approximations (like Hartree-Fock [28,31]). Direct diagonalization of small systems (lattices with $M = 6$ and 10 sites at half filling) with Coulomb interaction [26] yielded an (impurity) average persistent current that is suppressed by effects of the interactions except for strong disorder and weak interaction strength, where it is weakly enhanced. Direct diagonalization in one-dimensional rings of spinless fermions with short-range interactions in lattices of up to 20 sites [27] found that both, disorder and interactions, always decrease the persistent current by localizing the electrons. The above simulation deals with values of the disorder that are not strong in comparison with the typical kinetic energy of the electrons. Similar results have been obtained in this regime using the density matrix renormalization group (DMRG) method [30]. Hartree-Fock calculations also yielded a suppression of the persistent current as the strength of the interaction increases [28].

The conclusions that we extract from our numerical computations of the phase sensitivity are somehow different than that of the previous numerical studies. Working at large disorder, we find that when increasing the strength of the interactions, abrupt charge reorganizations of the many-body ground state take place (at sample-dependent values of the interaction strength) and are associated with anomalously large persistent currents [41–43]. In this work we extend our previous numerical calculations showing such an effect and we also present analytical work aiding towards its understanding. We point out to the importance of considering the physics of individual samples and we show that the delocalization effect of interactions persists in the thermodynamic limit.

A sizeable increase of the persistent current with the strength of the interaction had been obtained for moderately disordered 1D electronic systems *with spin* (Anderson-Hubbard model) from renormalization group approaches [23] or perturbation and numerical calculations [32]. Our results show that the spin does not seem to be a necessary ingredient to obtain an enhancement of persistent currents due to interactions. Even without spin, repulsive interactions can increase the persistent current, provided the disorder is important enough. This lets us expect an even more dramatic increase at strong disorder in models with spin.

It is interesting to remark that the enhancement of transport properties by the effect of a repulsive interaction has been proposed in other contexts than the one of this work. A system with strong binary disorder, where the two possible values of the disorder give rise to two separated bands, presents in the absence of interactions a gap if the filling is such that the lower band is filled completely [44]. Then, the broadening of the bands due to the interaction can lead to an overlap allowing for metallic behavior. Also, in a system of two interacting particles on a disordered chain it has been shown that the localization length is enhanced by the effect of interactions [45–48].

The remainder of the paper is organized as follows. In Section 2, we present the model and the numerical method. In Section 3, we perform numerical studies for the ground state structure and the phase sensitivity for the case of half filling. A scaling with the system size allows to demonstrate the delocalization effect of repulsive interactions in the presence of strong disorder. In Section 4, analytical work is presented, which aims to describe the basic physical mechanisms leading to the effects which were found numerically. In Section 5, we extend the numerical studies away from half filling and establish the criterium for observing a delocalization effect due to the interactions. Finally, we present in Section 6 our conclusions and outline some open problems.

## 2 Model and method

### 2.1 Model Hamiltonian

We consider spinless fermions on a chain with nearest-neighbor interaction

$$H = -t\sum_{i=1}^{M}(c_i^\dagger c_{i-1} + c_{i-1}^\dagger c_i) + \sum_{i=1}^{M} v_i n_i + U\sum_{i=1}^{M} n_i n_{i-1} \tag{9}$$

and twisted boundary conditions, $c_0 = \exp(i\Phi)c_M$. The operators $c_i$ $(c_i^\dagger)$ destroy (create) a particle on site $i$ and $n_i = c_i^\dagger c_i$ is the occupation operator. The on-site random energies $v_i$ are drawn from a box distribution of width $W$. The strength of the disorder $W$ and the interaction $U$ are measured in units of the kinetic energy scale ($t = 1$). The use of twisted boundary conditions allows to represent a ring of $M$ sites pierced by a flux $\Phi$.

### 2.2 Numerical method

The numerical results are obtained with the density matrix renormalization group (DMRG) algorithm [49,50]. In this method, successive iterations are obtained by

building larger (real space) blocks from smaller components. The Hamiltonian of each block can be diagonalized since in each iteration we truncate the states determined in the previous step. In the truncation process, states in the small blocks are selected as a function of their projection on the ground state of the larger block, and not as a function of their energies. The projection is computed from the reduced density matrix of the smaller blocks. The iteration of this procedure allows to calculate ground state properties in disordered 1D systems with an accuracy comparable to exact diagonalization, but for much larger systems [30].

It is important to recall that the eigenenergies of the many-body states of the disordered ring need to be obtained with large precision since the phase sensitivity is given as the difference of ground-state energies. We can typically achieve system sizes corresponding to 50 particles on 100 lattice sites by keeping up to 2000 states per block, and then the largest matrices that we have to diagonalize have a dimension of the order of 10 millions.

# 3 Half filling

We will center our numerical studies on the charge density and the $\Phi$-dependence of the ground state energy. We start in this section by treating the case of half filling (the number of electrons is $N = M/2$), leaving the case of an arbitrary filling for Section 5.

## 3.1 Charge reorganization in individual samples

### 3.1.1 Charge density

We start our analysis with the reorganization of the ground state induced by the nearest-neighbor (NN) repulsion (Fig. 1), plotting the charge density $\rho$ (expectation value of $n_i$) as a function of $U$ and site index $i$ for a typical sample ($M = 20$ and $N = 10$). In order to favor the inhomogeneous configuration, the disorder is taken large ($W = 9$) such that the localization length (a rough guess is given by the perturbative result for weak disorder $\xi_1 \approx 100/W^2$) is of the order of the mean spacing $k_F^{-1} = 2$ between the charges. For $U \approx 0$, one can see a strongly inhomogeneous density, while for large $U$ a periodic array of charges sets in. These two limits are separated by a sample-dependent crossover regime.

The charge reorganization can be clearly observed in the Fourier transform of $\rho$ with respect to the space variable $i$ (Fig. 2). For weak interactions the Fourier transform does not show significant structure. On the other hand, a single peak appears above a certain interaction strength, reflecting the establishment of a regular periodic array of charges. For intermediate interaction strengths, there is a tendency towards a periodic array, but defects persist and there are still several Fourier components present.
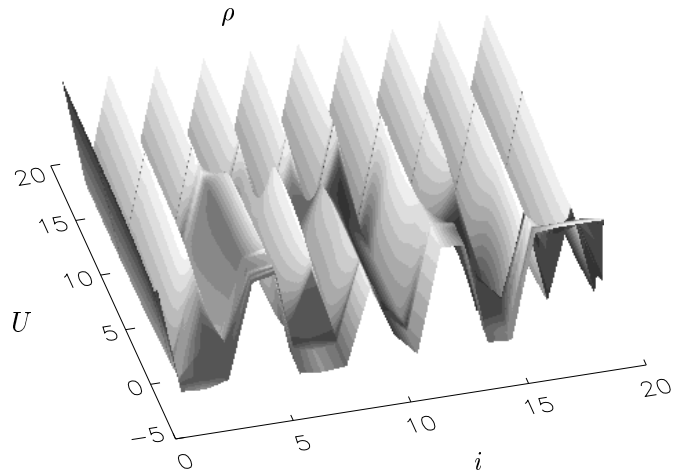


**Fig. 1.** Charge configuration for a typical sample (d of Fig. 3) for $N = 10$ particles on $M = 20$ sites at $W = 9$ as a function of the lattice site $i$ and the interaction strength $U$.
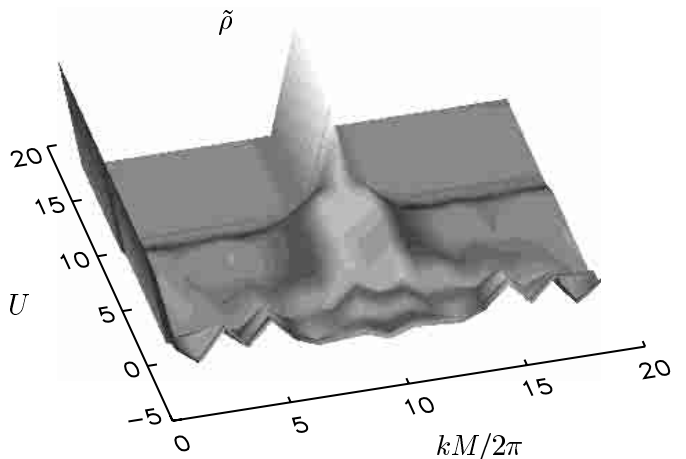


**Fig. 2.** Fourier transform of the charge configuration of Figure 1.

### 3.1.2 Density-density correlation function

In order to quantitatively describe the sample-dependent reorganization of the charge density, we calculate [42] the density–density correlation function

$$C(r) = \frac{1}{N} \sum_{i=1}^{M} \rho_i \rho_{i+r} \qquad (10)$$

for values $0 \leq r \leq M/2$. The parameter $\gamma = \max_r\{C(r)\} - \min_r\{C(r)\}$ is used to distinguish between the electron liquid with constant density ($\gamma = 0$), and the regular crystalline array of charges ($\gamma = 1$). Since we include the translation $r = 0$ in the definition of $\gamma$, we get $\gamma \neq 0$ for the electron glass. Thus, $\gamma$ measures charge crystallization from an electron liquid as well as the melting of the glassy state towards a more liquid ground state.

Figure 3 shows the dependence of $\gamma$ on the interaction strength for four individual samples representing different behaviors. For certain impurity configurations, like in sample a, the periodic array is obtained at a weak repulsive
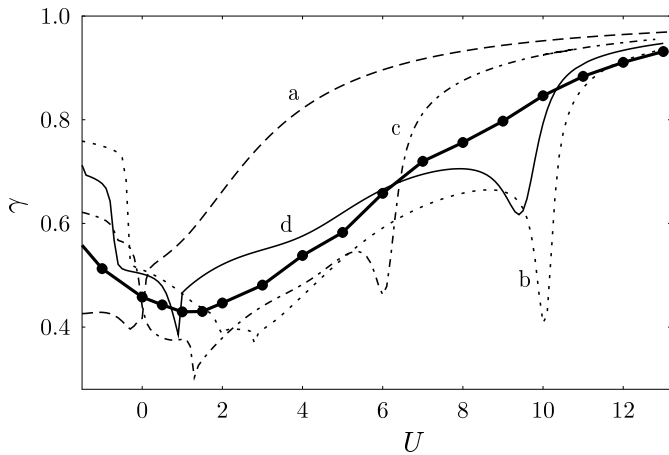
**Fig. 3.** Density–density correlation parameter $\gamma$ for four samples with $N = 10$, $M = 20$ and $W = 9$. Thick dots: Average over up to 166 samples.

interaction, while one needs a strong interaction for other samples like b and d. Typically, $\gamma$ assumes a minimum for a small repulsive interaction at a sample-dependent value $U_c$ of the order of the kinetic energy scale $t$. This means that the charge distribution is closest to a liquid around $U_c$ and suggests a maximum of the mobility of the charge carriers. This is an indication for a delocalization of the ground state by repulsive interactions. In addition, most of the samples show small steps in the interval $0 \leq U \leq 2t$, caused by instabilities between different configurations of similar structure. The formation of the regular array of charges imposed by strong repulsive interactions occurs at a sample-dependent interaction strength $U_m$. The step-like increase of $\gamma$ shows that the regular array is established abruptly at $U_m$.

Typically the first and last dips of $\gamma$ for repulsive $U$, signaling the above described charge reorganizations, are separated by a transition region. In order to describe our problem as a transition between phases we have to consider the average behavior of $\gamma$ and extract sample-independent values of the critical interaction strengths. The small dispersion of $U_c$ yields an average $\gamma$ presenting a minimum at an interaction strength $U_F$ of the order of $t$. This demonstrates the delocalization effect of a small repulsive interaction accompanied by a "more liquid" charge density. The increase of the persistent current in 1D models with spin was traced back to the effect of repulsive interactions making the charge density more homogeneous [23]. The present study shows that this mechanism also applies for spinless fermions in strongly disordered 1D chains.

Unlike the case of small $U$, for large interactions the jumps of $\gamma$ are widely spread and therefore smeared out in the ensemble average. Thus, starting from the sample-dependent values $U_c$ and $U_m$, it is possible to identify a sample-independent interaction strength $U_F$ associated with the first charge reorganization by the minimum of $\langle \gamma \rangle$, but the last charge reorganization does not give a clear signature on $\langle \gamma \rangle$. In the next subsection we give the

estimation of the typical interaction strength needed to establish the Mott phase. Recent works [13,51,52] on 2D disordered clusters with Coulomb interaction also shows that one goes from the Fermi glass towards the pinned Wigner crystal through an intermediate regime (located between two different Coulomb-to-Fermi energy-ratios $r_s^f$ and $r_s^w$). The difference with our problem is that, in the 2D case, a topological change can be observed in the pattern of the driven currents, which cannot exist in the 1D case. However, in the two problems, we are addressing the difficult question of the quantum melting of a solid array of charges (Mott insulator in our case, Wigner crystal for 2D Coulomb repulsion) in the presence of a random substrate. This melting can occur through a crossover regime (or an intermediate quantum phase in 2D) where a liquid of "defectons" may co-exist with an underlying solid background, as suggested by Andreev and Lifschitz [53].

### 3.1.3 Size dependence of the correlation parameter

The typical interaction strength needed to establish a perfectly regular array of charges can be estimated from the competition between interaction and potential energies in some special configurations. Starting from the perfect Mott configuration with alternating charges, we see that we can gain potential energy by going to configurations which are perfect only on parts of the lattice. The most favorable of this kind should typically be the case where the odd sites are occupied on half of the ring and the even sites on the other half of the ring, with two domain walls between these regions. The cost in interaction energy is $U$, while the gain in potential energy is of the order of $(W/2)\sqrt{N/2}$.

The periodic array over the whole system is favored when the cost of the defect is larger than the gain in potential energy. This typically happens for

$$U > U_W = \frac{W}{2}\sqrt{N/2}. \qquad (11)$$

At half filling ($N = M/2$), the critical interaction strength $U_W$ increases as the square root of the system size. In the dependence of the ensemble averaged correlation parameter on $U$ for different system sizes (Fig. 4) this tendency is clearly visible. The interaction scale on which $\langle \gamma \rangle$ increases to its maximum value 1, characterizing the Mott insulator, is shifted to higher interaction values when the system size is increased. In the thermodynamic limit, one expects that no finite interaction strength (provided it is short ranged) can be sufficient to impose a perfectly ordered Mott insulator in a disordered system, consistent with the findings of references [21,54].

### 3.2 Phase sensitivity and localization

In this section, we present calculations of the phase sensitivity of the ground state which is defined, in equation (8),
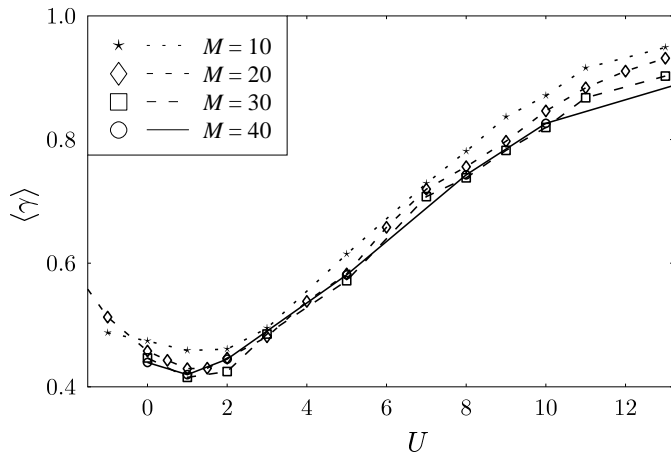
**Fig. 4.** Ensemble average of the density–density correlation parameter $\gamma$ as a function of the interaction strength for different system sizes $M$ at half filling and $W = 9$.



**Fig. 5.** Phase sensitivity $D(U)$ for four different samples with $N = 10$, $M = 20$, and $W = 9$ in (decimal) logarithmic scale. Thick solid line and dots: average of $\log(D)$.

as the energy difference between periodic ($\Phi = 0$) and anti-periodic ($\Phi = \pi$) boundary conditions. This phase sensitivity is a measure of the localization of the electronic wave-functions. The more insulating the system is, the weaker will be the effect of boundary conditions. As discussed in the introduction, the phase sensitivity conveys similar information, in the localized regime, as other measures of the response of the ground state to a flux threading the ring: the Kohn curvature [35] (charge stiffness) $\propto E''(\Phi = 0)$ and the persistent current $J \propto -E'(\Phi)$.

### 3.2.1 Phase sensitivity in individual samples

In Figure 5 we show the phase sensitivity $D(U)$ for the four samples presented in Figure 3, which were at half filling and with large disorder ($W = 9$). Both for $U \approx 0$ and $U \gg 1$, $D(U)$ is very small, but sharp peaks appear at sample-dependent values $U_\mathrm{c}$, where the phase sensitivity can be *4 orders of magnitude larger* than for free fermions. Remarkably, the curves for each sample do not present any singularity at $U = 0$ which could have allowed to locate the free fermion case (that appears simply as an intermediate case). Peaks can be seen at positive and negative values of $U$.

It is important to notice that each peak of $D(U)$ in an individual sample corresponds to a charge reorganization. This can be seen, directly, by following the evolution of the charge density as a function of $U$, or more systematically, by considering the one-to-one correspondence between the peaks of $D(U)$ and the dips of the density-density correlation parameter $\gamma$ (Fig. 3). The information of $D(U)$ and $\gamma(U)$ is complementary, but not equivalent: strong peaks of $D$ (happening for small values of $U$) correspond to small dips in $\gamma$, while the last charge rearrangement (leading to the Mott phase) is associated with a large dip in $\gamma$ and a small peak (or a shoulder) of $D$.

The free fermion case $U = 0$ corresponds to an Anderson insulator. A small repulsive interaction typically tends to delocalize the system and increases $D(U)$ until
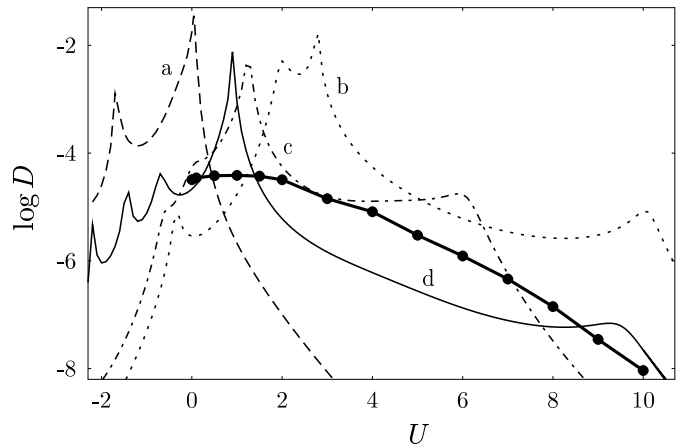
a charge reorganization takes place. In some cases (like sample a), the first charge reorganization for positive $U$ immediately drives the system to the homogeneous array of charges. In some other cases we go from the inhomogeneous density to the periodic array in a few steps signaled by additional peaks of the phase sensitivity. Examining the $U$ dependence of the density of those samples, one can note in some cases local defects in the periodic array subsisting up to large values of $U$. As discussed in Section 3.1.3, for a given interaction strength $U$, the appearance of defects becomes more and more likely as we increase the system size $M$ or the disorder $W$. Once the regular array of charges is established, the system becomes more and more rigid (pinned by the random lattice), and $D(U)$ decreases as a function of $U$. In Section 4.3 we calculate, by perturbation theory, the phase sensitivity of the Mott insulator in a disordered potential.

### 3.2.2 Mean values and statistics of the phase sensitivity

The critical values $U_\mathrm{c}$ of the interaction strength are sample dependent. Therefore, for a given value of $U$ we have a very different behavior for the samples where $U$ is close to a critical value than for those where it is not. Mixing the two situations leads to a widely fluctuating distribution of $D(U)$ and if we average logarithms, as usually done in the localized regime, we obtain the smooth curve of Fig. 5. We have checked that the probability distribution of D(U) is in fact log-normal (see insets of Fig. 7).

In Figure 6 we see that, for a given size and filling ($M = 20$, $N = 10$), the log-average $\langle \log D(U) \rangle$ increases while decreasing the disorder ($W = 9, 7$ and $5$). For $U = 0$ we have the usual non-interacting behavior, while for large $U$ the phase sensitivity becomes only weakly dependent on disorder (we will get back to this point in Sect. 4.3). We also see that $\langle \log D(U) \rangle$ decreases with the interaction strength $U$, except for small $U$ ($U \lesssim t$) and strong disorder ($W = 9$ and $7$). The regions for $U \approx t$, for $W = 9$ and $7$, are blown up in the insets (lower left and upper
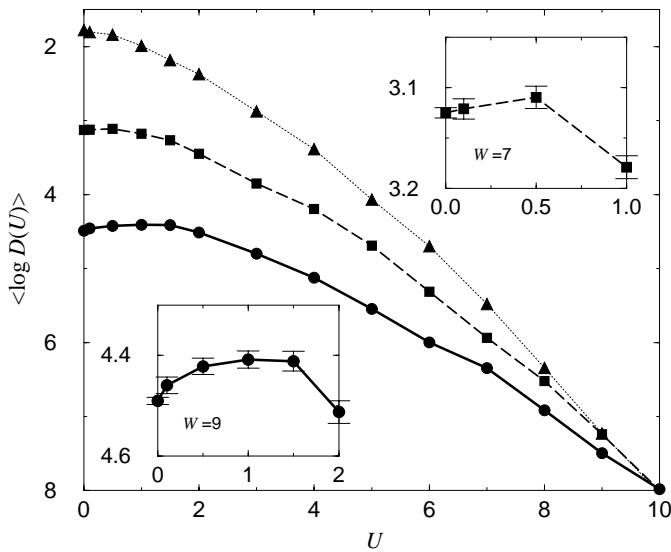
**Fig. 6.** Mean values of $\log D(U)$ for $M = 20$, $N = 10$ and three values of the disorder strength: $W = 5$ (triangles), $W = 7$ (squares) and $W = 9$ (circles). Upper and lower insets: blow up of the small-$U$ region for the last two cases showing a delocalization effect.



**Fig. 7.** Variance of the phase sensitivity as a function of $U$ for three values of the disorder strength: $W = 5$ (triangles), $W = 7$ (squares) and $W = 9$ (circles). Upper and lower insets: probability distribution (dots) of $\log D(0)$ and $\log D(2)$ respectively, calculated from 10 000 samples ($M = 20, N = 10, W = 9$). The mean values and variances are $\langle \log D(0) \rangle \approx -4.486$, $\sigma^2(0) \approx 1.49$ and $\langle \log D(2) \rangle \approx -4.495$, $\sigma^2(2) \approx 1.66$. The solid lines represent Gaussian distributions with these parameters.

right respectively), and show that the interaction scale for the first charge reorganization is weakly increasing with the disorder. The delocalization effect increases with the value of the disorder, but it is always very small. Our results for the average phase sensitivity are consistent with those of reference [26], finding a small increase of the average persistent current in small 1D systems (up to 5 electrons on 10 sites) by direct diagonalization. We show in our work that such an effect persists in larger systems and its small magnitude is to be contrasted with the spectacular enhancement found in individual samples.

The small delocalization effect on the average phase sensitivity together with the large sample-to-sample fluctuations makes it necessary to consider many impurity realizations (up to 5000) in order to confirm the enhancement beyond the statistical uncertainty. Comparing the information from Figures 3 and 6 we see that the average delocalization effect is more easily seen on the less fluctuating correlation parameter $\gamma$ than on $D$.

The widely fluctuating values of $D(U)$ can be represented to a very good approximation by a log-normal distribution for values of $U$ smaller than 8 (Fig. 7). The variances $\sigma^2(U) = \langle \delta(\log D(U))^2 \rangle$ are of the order of $|\langle \log D(U) \rangle|$. They increase slowly with $U$ in the region of $U \lesssim t$ (roughly the interval over which we see the delocalization effect), and more rapidly for larger values of $U$ (where the effect of the disorder becomes less important). Once the Mott regime is attained $\sigma^2$ no longer increases with $U$ (and becomes strongly dependent on $W$).

For a given sample the ratio between the phase sensitivity at a value of $U \neq 0$ and at $U = 0$ is also a widely fluctuating variable. Our numerical simulations (not shown) demonstrate that the variable $\eta = \log(D(U)/D(0))$ is normally distributed [41]. Such a behavior does not simply follow from the log-normal distributions for $D(U)$ and $D(0)$,
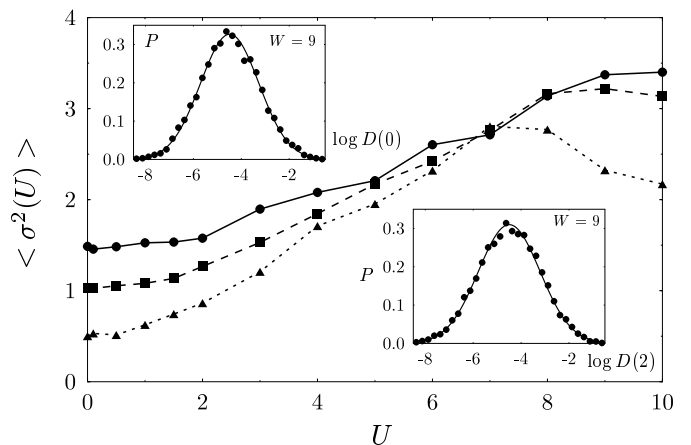
since these are not independent random variables. The width of the $\eta$-distribution is increasing with $U$, and for $U = 2$ variations of $D$ over more than an order of magnitude are typical [41]. The samples a and b shown in Figures 3 and 5 are characterized by extremely small and large values of $\eta$, respectively, while c and d are typical samples chosen around the center of the distribution.

### 3.2.3 Size dependence and thermodynamic limit

In the previous sections we described the increase of the phase sensitivity as a signature of the charge reorganizations that eventually lead to a Mott insulator upon increasing the interaction strength. On the other hand, as discussed in Section 3.1.3, in the thermodynamic limit the disorder will lead to defects in the Mott phase at any finite value of $U$. Two questions naturally arise at this point. Firstly, do charge reorganizations still exist and yield an enhancement of the phase sensitivity as we go to larger and larger systems? Secondly, will the delocalization effect survive in the thermodynamic limit?

In order to address the first question, we consider in Figure 8 the typical case of a sample with a strong disorder ($W = 7$). The actual realization of the impurity potential is sketched at the bottom panel (thick solid) for lattice sites going from $i = 1$ to $i = 40$. If we consider a sample of half such a size ($M = 20$) at half filling ($N = 10$) we obtain for the charge density (upper left panel) and for the phase sensitivity (filled squares, upper right panel) the kind of behavior previously discussed. A first charge reorganization takes place around $U = 1$ where a peak in $D(U)$ is observed. If we now consider the whole sample ($M = 40$) at the same filling ($N = 20$), $\log D(0)$ as well as the overall values of $\log D(U)$ are reduced by a factor of 2, but the
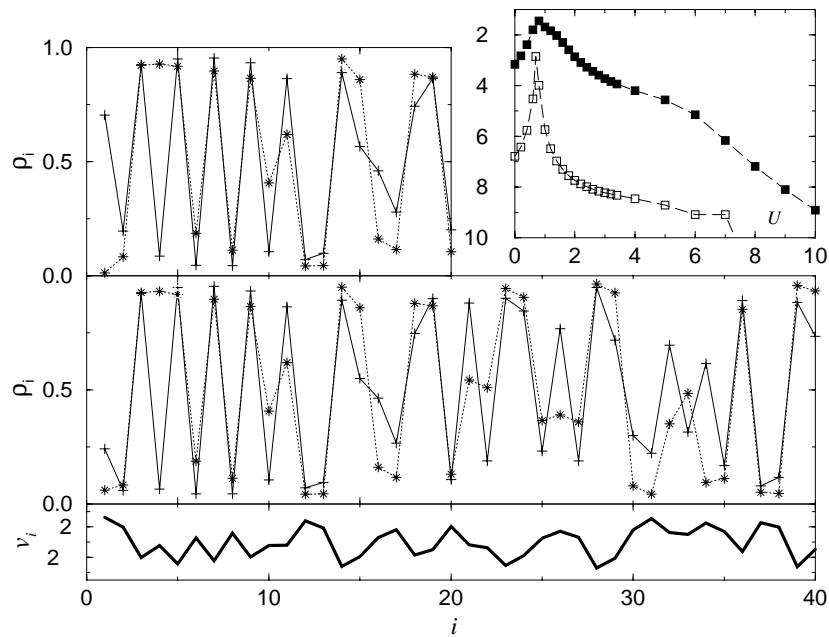
**Fig. 8.** Charge density as a function of the lattice site at half filling for a sample with $M = 20$, $N = 10$ (upper left panel) and with $M = 40$, $N = 20$ (central panel) with the impurity configuration $v_i$ represented by a thick solid line in the lower panel ($W = 7$). Stars and dotted lines correspond to $\rho_i(U = 0)$, while pluses and solid lines to $\rho_i(U = 3)$. In the upper right panel the (decimal) logarithm of the charge sensitivity as a function of $U$ is shown for the two samples: $M = 20$ (filled squares) and $M = 40$ (empty squares).

charge reorganization involving the first half of the sample still takes place (medium panel) giving rise to a sharper peak of $D(U)$ at a slightly shifted critical value (empty squares, upper right panel). This resonant-like behavior is generic. Upon increasing the sample size the peaks of $D(U)$ become sharper (and slightly shifted), and new charge reorganizations may yield supplementary structure in $D(U)$ (like the shoulder observed around $U = 7$).

Having answered the first question for the affirmative we still need to settle the second one, since it is not obvious that the sharper peaks yield a delocalization effect on the average. A detailed size-dependence study is needed, and we will focus on the interaction dependence of the localization length. In the absence of interactions, a 1D disordered system is an Anderson insulator, with the electron wave-functions localized on the scale of the one-particle localization length $\xi_1$. Then, the persistent current and the phase sensitivity scale with the system size $M$ proportional to $\exp(-M/\xi_1)$ [33].

For our many-particle system, the (many-body) localization length $\xi(U)$ depends on the interaction strength and can be defined from the scaling

$$\langle \ln D(U, M) \rangle = A(U) - \frac{M}{\xi(U)}, \qquad (12)$$

which in the non-interacting case ($U = 0$) yields the standard one-particle localization length characterizing the spatial decay of the electron wave-functions. The previous scaling is well satisfied in the accessible space of parameters [43] and allows to extract the values of $A(U)$ and $\xi(U)$. The former is weakly dependent on $U$ for $0 \leq U \leq 5$ and
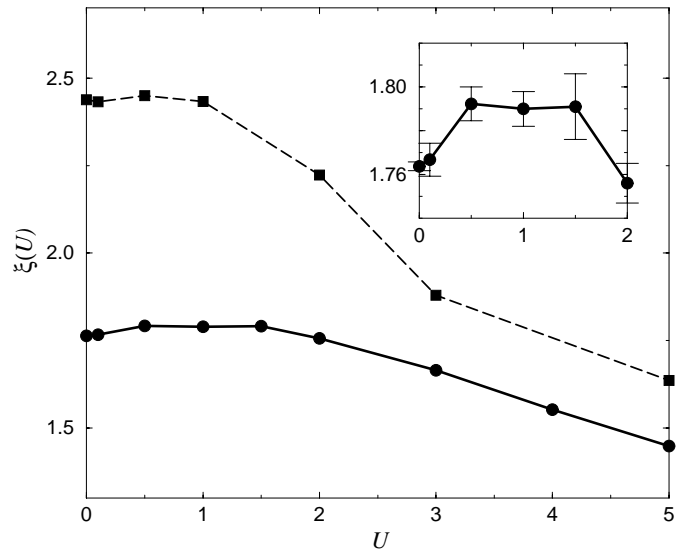


**Fig. 9.** Localization length obtained from the size-dependence of the phase sensitivity (Eq. 12) as a function of the interaction strength $U$ for half filling and two values of the disorder: $W = 7$ (squares) and $W = 9$ (circles). Inset: blow up of the small-$U$ region for the case of $W = 9$ showing a delocalization effect on $\xi$.

more strongly dependent for $U > 5$. The localization length exhibits a similar behavior as $\langle \log D(U) \rangle$. It decreases with the interaction strength except for small $U$ and strong disorder, where a small delocalization is observed (Fig. 9). For $W = 9$ (where the single-particle localization length is smaller than 2 lattice sites) a small repulsive interaction

results in a 2% effect on $\xi$, for $W = 7$ the delocalization effect is smaller, consistent with the behavior of $D(U)$. We therefore conclude that the delocalization on the average is not a finite-size effect.

# 4 Physical mechanisms

We have seen in the previous chapter how upon increasing the strength of the electron-electron interaction we go from the Anderson to the Mott insulating regimes through non-trivial transitions. In particular, our numerical simulations show that the intermediate regime is signed by charge reorganizations associated to an enhanced phase sensitivity. In this chapter we will try to understand the mechanism underlying such behavior and we will develop a perturbation theory yielding the phase sensitivity in the Mott regime in the presence of disorder.

## 4.1 Simplified model of two particles on three sites

The relation between charge reorganization and enhanced persistent current can be understood in a simple toy model of two particles (spinless fermions) on three sites. We consider the Hamiltonian of equation (9) with $M = 3$ and switch off the interaction between the extreme sites 1 and 3. Therefore, we write

$$H_{(3)} = -t \sum_{i=1}^{3}(c_i^{\dagger}c_{i-1} + c_{i-1}^{\dagger}c_i) + \sum_{i=1}^{3} v_i n_i + U \sum_{i=2}^{3} n_i n_{i-1}. \tag{13}$$

We keep the twisted boundary conditions, $c_0 = \exp(\mathrm{i}\Phi)c_3$ that allow us to address the phase sensitivity. The site-dependent interaction mimics the fact that in the large-$M$ case the sites 1 and 3 are joint through the rest of the chain (that we do not include in the description of the present model).

For two spinless fermions on three sites the Hilbert space has dimension 3 and the set $\{|1,1,0\rangle, |1,0,1\rangle, |0,1,1\rangle\}$ is a convenient basis specifying the occupation of the sites. We can readily diagonalize our $3 \times 3$ matrices for any value of our parameters $t$, $U$ and $v_i$. However, in order to simulate the localized regime we will only consider the case where at least one of the on-site potentials $v_i$ is much larger than the kinetic energy scale $t$. We then study the transition from $U = 0$ (where the potentials $v_i$ determine the charge distribution) to values of $U$ much larger than all the $v_i$ (where the ground state is mainly directed along the vector $|1,0,1\rangle$ in order for the electrons to avoid each other).

### 4.1.1 Three-site model with fixed impurity configuration

In a first step we further simplify our problem by restricting the disorder to $v_1 = v_2 = -\epsilon$ and $v_3 = \epsilon \gg t$. This

configuration clearly favors the state $|1,1,0\rangle$ at $U = 0$. In the two extreme cases the ground state energies are given by

$$E(U = 0) \simeq \left(-2\left(\frac{\epsilon}{t}\right) - \left(\frac{t}{\epsilon}\right) + \frac{1}{2}\left(\frac{t}{\epsilon}\right)^2 \cos\Phi\right)t, \tag{14a}$$

$$E(U \gg \epsilon) \simeq \left(-2\left(\frac{t}{U}\right) - 2\left(\frac{\epsilon t}{U^2}\right) + 2\left(\frac{t}{U}\right)^2 \cos\Phi\right)t, \tag{14b}$$

The term $-2\epsilon$ in equation (14a) is the on-site energy of the state $|1,1,0\rangle$, the next order terms in $t/\epsilon$ take into account the energy gain due to hopping. In the large-$U$ case there is no term in $\epsilon$ since the ground state is close to $|1,0,1\rangle$ and we have chosen $v_1 = -v_3$. From equations (14) we can calculate the phase sensitivity in the two limiting cases and obtain

$$D(0) \simeq \frac{3}{2}\left(\frac{t}{\epsilon}\right)^2 t \gg D(U \gg \epsilon) \simeq 6\left(\frac{t}{U}\right)^2 t, \tag{15}$$

in agreement with the fact that the phase sensitivity in the Mott phase is reduced with respect to that of the Anderson phase. However, the decrease of $D$ with $U$ is not monotonous; for the critical value $U_c = 2\epsilon$ we have a degeneracy that leads to an increased phase sensitivity:

$$D(U_c) \simeq \frac{3}{2}\left(\frac{t}{\epsilon}\right)t \gg D(0). \tag{16}$$

The enhancement factor $\eta = D(U_c)/D(0)$ is then given by

$$\eta = \epsilon/t = U_c/2t, \tag{17}$$

and even though both, $D(U_c)$ and $D(0)$ decrease when the disorder strength $\epsilon/t$ is increased, their ratio is increasing.

Our toy model then captures the physics of a charge reorganization associated with an enhanced sensitivity with respect to a perturbation at a point of degeneracy. The effect is reminiscent of the Coulomb blockade phenomenon. When the occupation numbers are approximately good quantum numbers (0 or 1) transport is blocked; in the transition between such extreme configurations the occupation numbers are no longer good quantum numbers and transport is favored. In the Coulomb blockade problem we have a true transport situation and the degeneracy is between the state having $N$ electrons in the dot and 1 in the leads with the state having $N+1$ electrons in the dot. Moreover, the constant charging energy model [55] allows us to think in terms of a one-particle problem. In our case we do not have a transport configuration but a delocalization of wave-functions and the degeneracy is between many-body ground states of the ring.

### 4.1.2 Disorder average in the three-site model

The result above for a given potential realization can be used to determine the ensemble average of the critical interaction strength $U_c$ within this toy model.

First of all, we relax the restriction to the disorder realizations, allowing for arbitrary on-site energies $v_i \in [-W/2, W/2]$, assuming box-distributions with probability density

$$P(v) = \frac{1}{W}\,\Theta(W/2 - |v|). \qquad (18)$$

For symmetry reasons, the exchange of the values $v_1 \leftrightarrow v_3$ leaves $D(U)$ unchanged and we consider always $v_1 > v_3$.

No level crossings between the ground state at $U = 0$ (adapted to the disorder configuration), and the ground state at $U \gg W$ (close to $|1, 0, 1\rangle$), occurs when the disorder realization favors the latter already at $U = 0$. This is the case if

$$v_2 > v_1, v_3, \qquad (19)$$

which is fulfilled in $1/3$ of the whole parameter space. Then, no positive $U_c$ exists within our toy-model, and no enhancement of $D(U)$ with respect to $D(0)$ can be expected for $U > 0$.

We now concentrate on the averaged enhancement factor $\langle \eta \rangle$, where the average is taken over the parameter space $v_2 < v_1$, in which an avoided level crossing occurs. In the absence of hopping ($t = 0$), the energies of the states $|0, 1, 1\rangle$ and $|1, 0, 1\rangle$ are given by $v_2 + v_3 + U$ and $v_1 + v_3$, respectively, such that a level crossing occurs at $U_c = v_1 - v_2$. Following the argument of the previous section, the hopping then leads to a $D(U)$ which is enhanced at $U_c$ by the factor $\eta = (v_1 - v_2)/2t$. The average over the part of the parameter space $(v_1, v_2, v_3)$ in which $v_2, v_3 < v_1$, using the box distributions yields

$$\langle \eta \rangle = \frac{3}{8}\frac{W}{t}\,. \qquad (20)$$

The average enhancement of the phase sensitivity increases proportionally to the disorder strength, as the average peak position, $\langle U_c \rangle = (3/4)W$. This behavior is consistent with our numerical findings for larger systems.

## 4.2 Avoided level crossings

In the toy model presented in the previous section we saw how an enhanced phase sensitivity is linked with a charge reorganization of the ground state. The charge reorganization took there a very simple form: at a certain critical value of the interaction strength an electron jumps from one site to its neighbor. Or, more precisely, the ground state that was, for small $U$, mainly given by the vector $|1, 1, 0\rangle$ became, after $U_c$, approximately aligned in the direction of $|1, 0, 1\rangle$. That can be seen as a crossing of two levels as a function of the parameter $U$. In this section we go back to our numerical simulations for large $M$ and demonstrate that the physics of level crossings is still valid despite the fact that the charge re-accommodation is not necessarily local (i.e. the electron may jump many sites across).
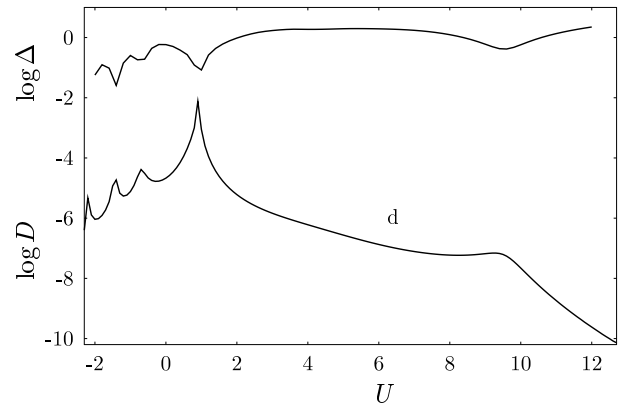


**Fig. 10.** The energy spacing $\Delta$ between the ground state and the first excited state of sample d of Figures 1, 3 and 5 (upper line) together with the corresponding phase sensitivity (lower line).

The sharp changes in the ground state structure and the peaks observed in the phase sensitivity are the consequences of avoided crossings between the ground state and the first excitation, obtained upon increasing $U$. While the ground state at weak interaction is well adapted to the disordered potential, another state with a different structure and better adapted to repulsive interactions, becomes the ground state at stronger interaction. In the case of large disorder, with a one-particle localization length $\xi_1$ which is of the order of the mean distance between the particles, the overlap matrix elements between the different noninteracting eigenstates due to the interaction are very small and the levels almost cross. There is only a very small interaction range where a significant mixing (hybridization) of two states is present. This is exactly where the peaks of the phase sensitivity appear.

This scenario is confirmed by Figure 10, where the phase sensitivity $D$ and the energy level spacing $\Delta$ between the ground state and the first excited state are shown as a function of $U$ for sample d. Here, we used the Lanczos algorithm for direct diagonalization in order to obtain the energies of a few excited states.

Minima of $\Delta$ appear at the interaction values of the peaks in the phase sensitivity. A gap of increasing size opens between the ground state and the first excitation after the last avoided crossing at interactions $U > U_m$, when the Mott insulator is established. A study of many other samples leads to the same conclusions. The statistics of the first excitation energy is therefore determining the behavior of the phase sensitivity. In 2D with Coulomb repulsion, this has recently been addressed giving rise to intermediate statistics [56] at the opening of the quantum Coulomb gap.

The importance of level hybridization in determining the persistent current of many-particle systems has also been demonstrated in reference [57] within a slightly different model: A ring enclosing a magnetic flux coupled to a side stub *via* a capacitive tunnel junction. In particular, it was shown that the passage through the hybridization point is associated with the displacement of charge in real

space, and also that strong enough Coulomb interactions can isolate the ring from the stub, thereby increasing the persistent current.

### 4.3 Phase sensitivity in the Mott insulator

#### 4.3.1 Perturbation theory in t/U

In the non-interacting limit, disorder leads to Anderson localization and the problem can be treated by an expansion in terms of $t/W$ [58]. In the Mott insulator limit, the interaction dominates, and it is possible to use an expansion in terms of $t/U$. In this second regime we decompose the Hamiltonian of equation (9) as

$$H = H_0 + H_1 \tag{21}$$

with an unperturbed part containing disorder and interaction

$$H_0 = \sum_{i=1}^{M} v_i n_i + U \sum_{i=1}^{M} n_i n_{i-1} \tag{22}$$

and the perturbation given by the hopping term

$$H_1 = -t \sum_{i=1}^{M} (c_i^\dagger c_{i-1} + c_{i-1}^\dagger c_i). \tag{23}$$

The solutions of the unperturbed part $H_0$ are simple. The eigenstates are products of on-site localized Wannier-states for each particle

$$|\psi_\alpha\rangle = \left( \prod_{k=1}^{N} c_{i_k(\alpha)}^\dagger \right) |0\rangle \tag{24}$$

($|0\rangle$ is the vacuum state) and the corresponding eigenenergies are given by

$$E_\alpha = \sum_{k=1}^{N} v_{i_k(\alpha)} + U N_{\text{NN}}(\alpha). \tag{25}$$

$N_{\text{NN}}(\alpha)$ is the number of particle-pairs in the configuration $\alpha$ which occupy nearest-neighbor sites.

It is important to notice that, in contrast to $H_0$, the perturbing part $H_1$ depends on the boundary condition $c_0 = \exp(\mathrm{i}\Phi)c_M$. For periodic (p, $\Phi = 0$) and anti-periodic (ap, $\Phi = \pi$) boundary conditions one obtains

$$H_1^{\text{p}} = -t \sum_{i=2}^{M} (c_i^\dagger c_{i-1} + c_{i-1}^\dagger c_i) - t(c_1^\dagger c_M + c_M^\dagger c_1) \tag{26}$$

and

$$H_1^{\text{ap}} = -t \sum_{i=2}^{M} (c_i^\dagger c_{i-1} + c_{i-1}^\dagger c_i) + t(c_1^\dagger c_M + c_M^\dagger c_1), \tag{27}$$

respectively.

The $n$th order correction to the phase sensitivity is given by

$$D_n(U) = (-1)^N \frac{M}{2} (E_n^{\text{p}} - E_n^{\text{ap}}), \tag{28}$$

where $E_n^{\text{p}}$ and $E_n^{\text{ap}}$ are the $n$th order terms in the perturbation expansion of the ground state energies for the Hamiltonians $H_1^{\text{p}}$ and $H_1^{\text{ap}}$, respectively.

#### 4.3.2 Phase sensitivity without disorder

The result for the problem without disorder has already been mentioned in the literature [29]. We present here its derivation and generalize it to the case with disorder. In the limit $t/U = 0$, the ground state of our Hamiltonian at half filling is given by a regular array of charges without nearest-neighbor sites simultaneously occupied. There are two possibilities to realize such an array, either all the particles seat on the odd sites of the chain

$$|\psi_0^{\text{o}}\rangle = \left( \prod_{k=1}^{N} c_{2k-1}^\dagger \right) |0\rangle, \tag{29}$$

or the $N$ particles are on the even sites

$$|\psi_0^{\text{e}}\rangle = \left( \prod_{k=1}^{N} c_{2k}^\dagger \right) |0\rangle. \tag{30}$$

These states both have zero energy and therefore, in order to study the effect of the boundary conditions, we have to use degenerate perturbation theory in the subspace spanned by $|\psi_0^{\text{o}}\rangle$ and $|\psi_0^{\text{e}}\rangle$. For each boundary condition, we can build the perturbation expansion in $t$ from the matrix elements

$$\mathcal{H}_n^{\text{s,s}'} = \tag{31}$$
$$\sum_{\alpha_1, \alpha_2, \dots, \alpha_{n-1}} \frac{\langle \psi_0^{\text{s}} | H_1 | \psi_{\alpha_1} \rangle \langle \psi_{\alpha_1} | H_1 | \psi_{\alpha_2} \rangle \dots \langle \psi_{\alpha_{n-1}} | H_1 | \psi_0^{\text{s}'} \rangle}{(E_0 - E_{\alpha_1})(E_0 - E_{\alpha_2}) \dots (E_0 - E_{\alpha_{n-1}})},$$

with s, s' = {o, e} and $H_1$ given by $H_1^{\text{p}}$ or $H_1^{\text{ap}}$ depending on the value of $\phi$ (0 or $\pi$, respectively). The sums run over all the eigenstates $\alpha$ of $H_0$ except the two degenerate basis states (29) and (30). There are two different types of matrix elements: the diagonal ones ($\mathcal{H}_n^{\text{e,e}}$ and $\mathcal{H}_n^{\text{o,o}}$, starting and finishing at $|\psi_0^{\text{e}}\rangle$ and $|\psi_0^{\text{o}}\rangle$, respectively), and the off-diagonal ones ($\mathcal{H}_n^{\text{o,e}}$ and $\mathcal{H}_n^{\text{e,o}}$, starting and ending at different states).

The numerators of equation (31) contain matrix elements $\langle \psi_{\alpha_i} | H_1 | \psi_{\alpha_{i+1}} \rangle$ of the perturbing Hamiltonian. Since $H_1$ consists of one-particle hopping terms, non-zero matrix elements can arise only if the two states $|\psi_{\alpha_i}\rangle$ and $|\psi_{\alpha_{i+1}}\rangle$ differ by nothing else than the position of one of the particles. In addition, since the hopping terms allow only hopping to adjacent sites and we are dealing with spinless fermions, the order of the particles on the chain is conserved in the subsequent hoppings.
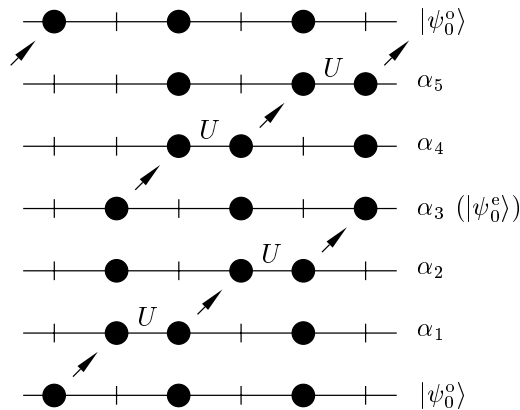
**Fig. 11.** A lowest order sequence contributing to the phase sensitivity for the example of $N = 3$ and half filling.

In Figure 11 we sketch a sequence of states $\alpha$ connecting $|\psi_0^{\text{o}}\rangle$ with itself for an $n = 6$ diagonal contribution. The first three steps of the sequence, connecting $|\psi_0^{\text{o}}\rangle$ and $|\psi_0^{\text{e}}\rangle$, represent an off-diagonal contribution to $n = 3$. We indicate with $U$ the interaction energy associated with each of the intermediate states of the sequence. Generally, the sequences in the states $\alpha$ can go "forward" and/or "backwards". For instance, a possible term contributing to $n = 2$ is that in which after the state $\alpha_1$ we go directly back to $|\psi_0^{\text{o}}\rangle$. However, since we are interested in the difference between periodic and anti-periodic boundary conditions, it is only the $\phi$-dependent terms that are relevant. That is, those involving a hopping between the sites $M$ and 1.

In the case of periodic boundary conditions all the hopping terms have a negative sign. Thus, the numerators appearing in equation (31) are proportional to $(-t)^n$. For anti-periodic boundary conditions the numerators are proportional to $(-t)^n(-1)^{h_b}$, where $h_b$ is the number of hoppings across the boundary between the sites $M$ and 1. Therefore, the corrections to the ground state energy due to the presence of finite hopping are the same for both boundary conditions, except for the contributions to the sums with odd $h_b$. These last contributions are the only ones relevant for the finite phase sensitivity.

The sequences with $n < N$ yield vanishing non-diagonal matrix elements, since we need at least $N$ hoppings to go between $|\psi_0^{\text{o}}\rangle$ and $|\psi_0^{\text{o}}\rangle$. In the diagonal matrix elements with $n < M$ the sequences are such that each particle returns to its starting point, by doing forward and backward hoppings, and therefore $h_b$ is necessarily even. Thus, these diagonal matrix elements are independent on the boundary condition, and in addition $\mathcal{H}_n^{\text{o,o}} = \mathcal{H}_n^{\text{e,e}}$ (the denominators do not depend on the boundary condition, nor on the initial state).

The above described behavior of diagonal and non-diagonal matrix elements shows that the degeneracy is not lifted for $n < N$. The lowest order in the perturbation expansion which lifts the degeneracy, and at the same time yields a contribution to the phase sensitivity, is $n = N$. For this order of the perturbation we have finite non-diagonal matrix elements given by sequences where each of the par-

ticles is moved by one site, the final state being the other basis state of the degenerate subspace. The connection between the two states $|\psi_0^{\text{o}}\rangle$ and $|\psi_0^{\text{e}}\rangle$ can be done by a sequence where all the particles hop forward, and also by a sequence of backward hoppings. If one of these two sequences crosses the boundary (yielding $h_b = 1$, changing the sign in the case of anti-periodic boundary conditions), the other does not (yielding $h_b = 0$).

For the sequences that go between $|\psi_0^{\text{o}}\rangle$ and $|\psi_0^{\text{e}}\rangle$ crossing the boundary, *either with periodic or anti-periodic boundary conditions*, we have to consider an additional sign $(-1)^{N-1}$ arising from the permutations needed to recover the initial ordering of the fermionic operators in the final state. For an odd number of particles $N$ and anti-periodic boundary conditions, the contributions of the forward and backward sequences cancel each other and $\mathcal{H}_N^{\text{o,e}} = \mathcal{H}_N^{\text{e,o}} = 0$, while with periodic boundary conditions both sequences add and we have non-zero off-diagonal matrix elements that lift the degeneracy. For an even number of particles, the opposite behavior occurs: The non-zero off-diagonal matrix elements are those corresponding to anti-periodic boundary conditions. In this way there is a difference between periodic and anti-periodic boundary conditions for all possible values of $N$. The corrections to the ground state energies are given by the lowest eigenvalue of the matrices $\mathcal{H}_N$. Since the diagonal matrix elements are the same, and independent of the boundary conditions, for odd $N$ we have $E_N^{\text{p}} - E_N^{\text{ap}} < 0$, and for even $N$ we have $E_N^{\text{p}} - E_N^{\text{ap}} > 0$. These signs ensure that $D_N$ is positive, in agreement with a general theorem proposed by Leggett [37] and the result for a Luttinger liquid [38], fixing the sign of $E^{\text{p}} - E^{\text{ap}}$ according to the parity of the number of electrons.

The splitting of the energy levels (and therewith the phase sensitivity) is given by the size of the off-diagonal matrix elements, which we estimate in the sequel. At half filling, the ground state configurations are the only ones which do not contain any nearest-neighbor sites simultaneously occupied, and their interaction energy vanishes. The eigenenergies of the excited states of $H_0$ are $E_\alpha = U, 2U, 3U \ldots$, depending on the number of particles placed next to each other. Thus, the absolute values of the denominators in equation (31) are of the order $U^{n-1}$. We have shown that the numerators are of order $t^n$, therefore, the parametric dependence of the lowest order ($N$th) correction to the phase sensitivity is given by

$$D_N(U) \propto U \left(\frac{t}{U}\right)^N \tag{32}$$

with an $M$-dependent prefactor, in agreement with the result mentioned by Tsiper and Efros [29]. Since higher order ($n > N$) terms contain higher powers of $t/U$, the result (32) is the leading correction in the limit of strong interaction $t/U \ll 1$.

### 4.3.3 Phase sensitivity with disorder

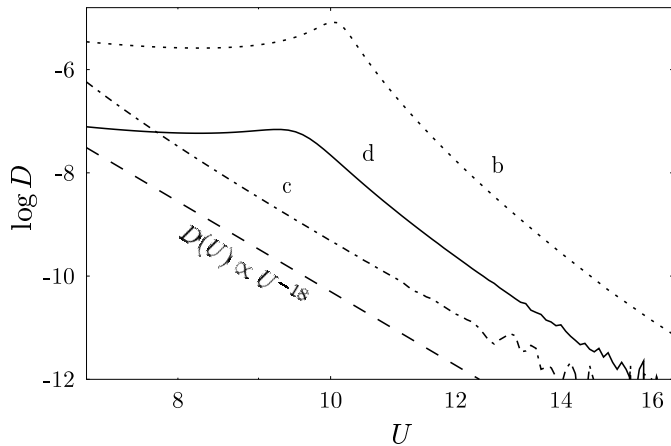The Mott insulator survives the introduction of disorder only for finite-size samples and not too strong disorder

**Fig. 12.** The dependence of the phase sensitivity on the interaction strength for the samples b,c, and d of Figures 3 and 5, at half filling ($N = 10$, $M = 20$, $W = 9$), in double-logarithmic representation. Sample a exhibits the same asymptotic power law, but with a much smaller prefactor such that the corresponding curve lies outside the scale of the figure. The dashed line shows the perturbatively predicted slope $D(U) \propto 1/U^{2N-2}$.

such that $U > W\sqrt{N}$. We will place ourselves in this regime in order to calculate perturbatively the phase sensitivity. The analysis presented for the clean case must be modified, and leads to a qualitatively different result. First of all, the two different possibilities to realize the regular array of charges will still be the energetically lowest configurations in the limit of strong interaction $U \gg t, W$, but the two states $|\psi_0^o\rangle$ and $|\psi_0^e\rangle$ are no longer degenerate. Their energies at $t = 0$ are given by

$$E_{\text{odd}} = \sum_{k=1}^{N} v_{2k-1} \qquad \text{and} \qquad E_{\text{even}} = \sum_{k=1}^{N} v_{2k}, \qquad (33)$$

respectively, and differ typically by $W\sqrt{N}$. If this difference is much larger than their coupling due to the hopping terms (which, according to a perturbative argument like the one presented above, is of the order of $t^N/U^{N-1}$), the ground state is given by one of the two base states, but not by a superposition of them. For $N$ sufficiently large, or in the limit of large $U$ where we are working, this is always true.

As a consequence, one can use standard non-degenerate perturbation theory and only sequences of hopping terms with $h_b \neq 0$ which connect the ground state to itself can give rise to a phase sensitivity. The lowest order contribution to the phase sensitivity must include now $M = 2N$ hopping terms to translate each of the particles starting at odd (or even) sites by two sites such that the final configuration is equal to the initial one. This sequence contributes in equation (31) to the diagonal matrix element, connecting the ground state ($|\psi_0^o\rangle$ or $|\psi_0^e\rangle$) with itself, proportionally to $(-t)^M(-1)^{N-1}$ in the case of periodic boundary conditions. In the case of anti-periodic boundary conditions we must add a sign $(-1)$ associated with the *one* traversal of the boundary. In contrast to the

clean case, forward and backward sequences always cross the boundary and yield contributions of the same sign to the diagonal matrix elements. Since the denominators do not depend on the boundary conditions, the difference $E_M^p - E_M^{ap}$ has the correct sign [37] to yield a positive $D_M$.

As illustrated in Figure 11, one of the intermediate states can be the regular array with the opposite parity than the initial state. The energy difference associated to this state is not $U$ (like for all the other intermediate states with nearest-neighbor sites occupied) but $|E_{\text{odd}} - E_{\text{even}}|$. The denominator containing the lowest power of $U$ is then of the order $WU^{2N-2}$ yielding

$$D_{2N}(U) \propto U \left( \frac{U}{W} \right) \left( \frac{t}{U} \right)^{2N}, \qquad (34)$$

as the dominating behavior when $U \gg t, W$. This is verified in our numerical simulations (Fig. 12) when considering individual samples after their last charge reorganization. The weak dependence with respect to $W$ can be seen from the large-$U$ behavior in Figure 6.

### 4.3.4 Localization length for the Mott insulator

From the exponential size-dependence of equations (32) and (34), one can extract the localization length in the Mott insulator. Imposing the size scaling of equation (12) we obtain for large $M$ a localization length

$$\xi_{\text{clean}} = 2 \left( \ln \left( \frac{U}{t} \right) \right)^{-1}, \qquad (35)$$

in the clean case, while with disorder we have

$$\xi_{\text{dirty}} = 1 \left( \ln \left( \frac{U}{t} \right) \right)^{-1}. \qquad (36)$$

Both typical lengths shrink with increasing interaction strength. Interestingly, the presence of disorder reduces the localization length of the Mott insulator to one half of the clean value, independent of the disorder strength $W$. It is important to recall that the size-dependence that yields the typical length $\xi_{\text{dirty}}$ of equation (36) has to be restricted to the condition $U > W\sqrt{N} > t^N/U^{N-1}$, allowing $N$ to vary over several orders of magnitude when $U$ is large. $\xi_{\text{dirty}}$ describes the exponential decrease of $D$ with the system size within this range.

The logarithmic dependence of the localization length on the interaction parameter is also found for the Hubbard model in a clean one-dimensional system [59] as well as in a disordered 2D model with Coulomb repulsion [60].

## 5 Dependence on filling

In the previous sections we have been mainly concerned with the interaction effects of spinless fermions at half filling. At half filling, and with strong disorder, a short-range
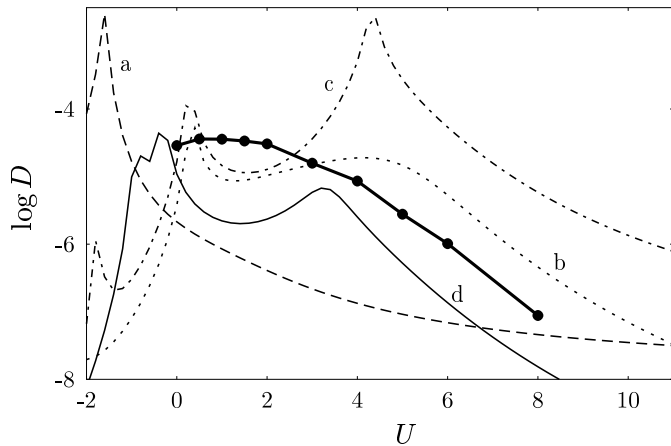
**Fig. 13.** Phase sensitivity $D(U)$ for four samples with the impurity configurations of those of Figure 5, but with only $N = 9$ particles ($M = 20$, $W = 9$). The average over many samples is represented by the thick dots.

interaction has a dramatic effect on the charge density. We have seen that reducing the disorder increases the localization length and results in less important charge reorganizations. Reducing the electron density increases the inter-particle distance, making a short-range interaction less effective. In this section we analyze the effect of short-range interactions as we move away from the optimal conditions of strong disorder and half filling.

## 5.1 Fillings close to one half

In Figure 13 we present the phase sensitivity for strong disorder ($W = 9$) and a filling close to one half ($N = 9$, $M = 20$). In analogy with the case of half filling presented in Figure 5, we see strong peaks of $D$ for individual samples and a broad maximum for the average values (thick dots). We therefore confirm that the physics of charge reorganizations is robust, and it is not a simple commensurability effect restricted to half filling.

## 5.2 Phase sensitivity in the large-U limit

The similarities between Figures 5 and 13, that we have pointed out above, concern the charge reorganizations and the corresponding peaks of $D$ for relatively weak interactions (of the order of $t$). In the large-$U$ limit there appear some differences between the cases of half filling and less than half filling. For instance, we can see a tendency towards saturation of $D(U)$ for the samples a and c of Figure 13. In fact, in a larger $U$-range we observe that all the curves for densities less than one half saturate for sufficiently large $U$.

This saturation is easy to understand from the perturbative analysis given in Section 4.3. In the sequence of intermediate states $|\psi_\alpha\rangle$ contributing to each of the terms in equation (31) (one of them represented in Fig. 11) we readily see that at less than half filling it becomes possible

to move the particles one after the other on the chain without ever having two particles on neighboring sites. These sequences give boundary condition dependent contributions to $E_n$ without any dependence on $U$ in the denominators ($E_0 - E_{\alpha_i}$). Since they are the only contributions which survive in the large-$U$ limit, they define the value at which the phase sensitivity saturates.

The same happens at more than half filling, when already the ground state contains the minimum number $2N - M$ of nearest neighbors. Here, it is possible to translate all of the particles at constant interaction energy thereby leaving $U$-independent contributions to (31).

## 5.3 Charge reorganization at high disorder

Repulsive interactions give rise to charge reorganizations when the non-interacting ground state fixed by the disorder configuration is not well adapted (energetically) to a finite value of $U$. Assuming a very strong random potential, such that the one-particle states are close to on-site Wannier states, the ground state of $N$ particles on $M \geq 2N$ sites (more than half filling can be treated similarly, using the particle-hole symmetry) at $U = 0$ is given by the particles occupying the $N$ lowest sites. The positions of these $N$ sites on the ring are random. No reorganization of the ground state due to short-range repulsive interaction takes place when this configuration does not contain any two particles on neighboring sites.

The probability for obtaining such a configuration can be calculated as follows. One starts from the configuration where the particles occupy the $N$ first odd sites of the ring $\{1, 3, \ldots, 2N-1\}$ and each of the particles has 'his' empty even site on its right. Then, $M - 2N$ empty sites are still available which can be distributed among the $N$ gaps on the right hand side of the particles, and we obtain

$$\Omega = \frac{M}{N} \begin{pmatrix} M - N - 1 \\ M - 2N \end{pmatrix} \tag{37}$$

different possible configurations without nearest neighbors. The factor of $M/N$ arises because of the $M$-fold translational symmetry of the problem and the indistinguishability of the $N$ particles.

Since the total number of possibilities to place $N$ spinless fermions on $M$ sites is given by

$$T = \begin{pmatrix} M \\ N \end{pmatrix}, \tag{38}$$

the probability to have a configuration without nearest neighbors in a given sample is

$$P = \frac{\Omega}{T} = \frac{M}{N} \frac{\begin{pmatrix} M - N - 1 \\ M - 2N \end{pmatrix}}{\begin{pmatrix} M \\ N \end{pmatrix}}. \tag{39}$$

Introducing the filling factor $x = N/M$, and using Stirling's approximation for the evaluation of the
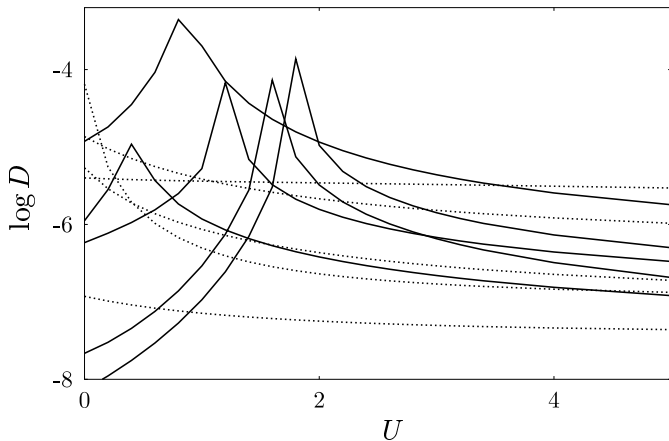
**Fig. 14.** Phase sensitivity for ten samples with quarter-filling ($N = 5$, $M = 20$) and strong disorder ($W = 9$). Roughly half of the samples exhibit a peak in $D(U)$ (solid lines), while the other half yield a monotonously decreasing phase sensitivity.



**Fig. 15.** Thin lines: three samples (a, b and c) with $M = 40$, $N = 10$ and $W = 4$. Thick lines: three samples (a', b' and c') with $M = 40$, and $N = 10$ obtained by scaling the previous impurity potentials from $W = 4$ to $W = 5$. Thick solid line and dots: average of $\log(D)$ for $W = 5$.

factorials, we find

$$P \simeq e^{Mg(x)} \quad \text{with} \quad g(x) = \ln\left(\frac{(1-x)^{2(1-x)}}{(1-2x)^{(1-2x)}}\right). \quad (40)$$

Since $g(x)$ is negative for all $0 < x \leq 1/2$, we obtain always $P = 0$ in the thermodynamic limit $M \to \infty$ at constant filling $x$. Therefore, *in the case of strong disorder* ($W \gg t$), the probability to obtain a charge reorganization due to repulsive interactions is one in the thermodynamic limit, at arbitrary filling.

In Figure 14 we consider the case of strong disorder ($W = 9$) and quarter filling ($M = 20$, $N = 5$). For large $U$ we observe the saturation of $D(U)$ described in the previous chapter. In the regime of smaller $U > 0$ we observe samples for which there is a peak in $D(U)$ (exhibiting also a charge reorganization) and others in which $D(U)$ is a monotonously decreasing function. In the former case the $U = 0$ configuration has nearest-neighbor sites that are occupied, while in the latter there is no occupancy of nearest neighbors in the non-interacting problem, and by increasing $U$ we do not achieve any substantial charge reorganization. A systematic study over many samples with the conditions of Figure 14, yields a probability of about 0.5 to obtain a sample which does not present a peak in $D(U)$, while equation (39) predicts $P \approx 0.26$. This discrepancy can be traced to the fact that equations (39) and (40) are valid in the limit of a very strong disorder $W \gg t$. For the parameters used in Figure 14 it is not always true that the $N$ particles occupy the $N$ sites with lower electrostatic potential, since the non-zero kinetic energy can split the two levels associated with two neighboring sites if their on-site energies are closer than $t$ (*i.e.* when a local potential well is formed by two nearly-degenerate sites). This splitting reduces the probability to have two adjacent sites occupied in the non-interacting ground-state.
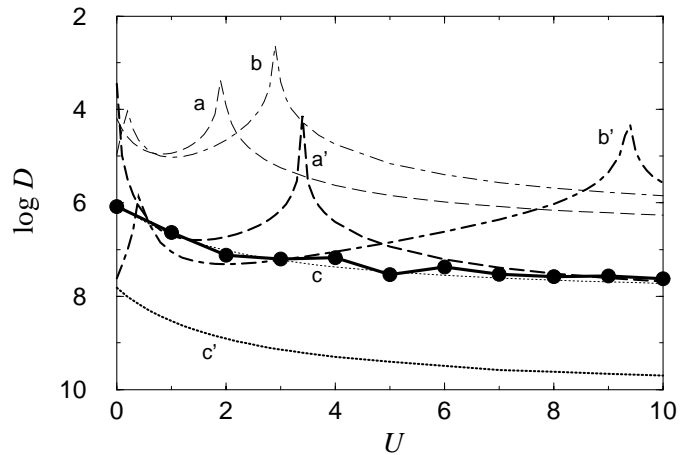
### 5.4 Low fillings - weak disorder

We have analyzed above the limit of very strong disorder, when the one-particle states are almost completely localized on one of the sites. We have seen that in this regime a short-range interaction leads to a charge reorganization whenever two neighboring sites are occupied at $U = 0$. Therefore, in finite size samples, the probability of having peaks in $D(U)$ is maximum at half filling. At weaker disorder, and without interaction, the particles are localized over several sites. The occupation of a site is no longer an almost good quantum number (0 or 1) and turning on a short-range interaction does not always result in a charge reorganization.

In Figure 15 we present the case of quarter filling ($N = 10$, $M = 40$) for three samples (a, b and c) with a disorder $W = 4$, and another three samples (a', b' and c') obtained from the first ones by scaling the impurity potentials to $W = 5$. For instance, the configurations of samples a and a' are obtained from the same set of random numbers, and it is only the overall scale of the fluctuations that changes. For certain samples (like c) the non-interacting system has all the electrons localized far away from each other and the charge configuration does not change when turning on the interactions, resulting in a monotonously decreasing $D(U)$. On the other hand, in other samples (like a and b) the non-interacting one-particle wave functions overlap considerably and the appearance of a short-range interaction results in a charge reorganization. In all cases we appreciate the saturation of $D(U)$ for large $U$, as discussed in 5.2.

Going from $W = 4$ to $W = 5$ for each of the samples changes the details of the curves, but not their nature. For instance, the peaks of a' and b' are obtained for stronger interactions than those of a and b. Such a behavior is understandable since higher disorder within the same random configuration necessitates a stronger interaction to

produce a charge reorganization. If we keep increasing $W$ for a sample exhibiting a peak, we obtain sharper resonances at increasing values of the interaction. Of course, for all samples, the typical values of $D$ are reduced when increasing $W$. Decreasing the disorder below $W = 4$ results in broader peaks, that disappear once the localization domain of the individual wave-functions becomes of the order of the inter-particle distance. The presence of peaks in the phase sensitivity is therefore fixed by the impurity configuration of the sample, and independent of the strength of the disorder in some range of $W$.

The different behaviors obtained among the samples with a given value $W$ of the disorder are responsible for the fact that the average phase sensitivity ($\langle \log D(U) \rangle$, thick dots in Fig. 15) decreases monotonously with the interaction strength, instead of exhibiting the broad maximum obtained for half filling and high disorder. We have seen that in the limit of very strong disorder it was possible to give a crude estimation of the probability to have a sample that presents a peak in $D(U)$. Once the disorder is weak enough to have single-particle states localized over several sites, we know that such a probability decreases, but it is rather difficult to extend the previous analysis in order to give an estimation of it. The relevant parameters are the one-particle localization length $\xi_1$, fixed by the disorder, and the inter-particle distance $1/k_F$, fixed by the electron filling. As a function of these two parameters we can clearly distinguish two cases:

(i) When $\xi_1$ becomes much smaller than $1/k_F$, the charge density without interaction in finite size samples is more and more likely to consist of $N$ distant peaks. Since such configurations are well adapted to the interacting case as well, the probability to find reorganizations of the ground state due to the interaction is reduced.

(ii) In the opposite case, when $\xi_1$ becomes much larger than $1/k_F$, no distinct one-particle peaks are present in the charge density at $U = 0$, and there are no regions of the sample with very small charge density. While increasing $U$, the total energy is minimized by gradually pushing the particles away, but there are no sudden charge reorganizations accompanied with peaks of the phase sensitivity. This behavior leads to a smooth decrease of $D(U)$.

Between the two previous cases, we find the optimal situation, $k_F \xi_1 \approx 1$, to observe the delocalization effect of interactions. This rough criterium is based on mean values (filling $N/M$ and disorder $W$) and only fixes the probability to obtain peaks in $D(U)$. The occurrence, or not, of charge reorganizations depends on the specific sample. That is, on the random configuration of the impurity potential. We have seen that if a given sample exhibits a peak of $D(U)$, such a behavior is maintained over some range of values of the disorder $W$ (small enough not to take us away from the condition $k_F \xi_1 \approx 1$ and into the limits (i) and (ii) previously discussed). It is worth to notice that the disappearance of charge reorganizations, that we obtain upon decreasing the disorder or the electron density, are tightened to the fact that we work with repulsive nearest-neighbor interactions. A long range interaction could be effective in yielding charge reorganizations away from the optimal conditions of half filling and strong disorder.

# 6 Conclusions

We have investigated spinless fermions in strongly disordered chains, as a function of the strength of a short-range repulsive interaction, mainly for densities corresponding to half filling. Such a system is a Fermi glass (Anderson insulator) for small values of the interaction (when the disorder is the dominant energy scale), and a Mott insulator when the interaction dominates over the disorder. Using a powerful numerical method, the density matrix renormalization group algorithm, we have been able to address the transition regime between these two previous limits, which is not accessible by perturbation theory or mean field approaches. We have calculated the charge density of the many body ground state, as well as the dependence of the ground state energy on the boundary condition. This last property, quantified by the so-called phase sensitivity, is related to the transport properties and also to the persistent current in the chain. It has a small finite value for the Anderson insulator and decreases with increasing interaction strength in the Mott insulator.

In striking contrast to the case of weak disorder, where repulsive interactions always strengthen localization for spinless fermions in one dimension, we have shown that in strongly disordered samples, and close to half filling, the ensemble average of the phase sensitivity can be enhanced by a repulsive interaction $U$. It shows a maximum at a value $U_F \approx t$, that is, for interaction strengths of the order of the kinetic energy scale. The study of the density-density correlations reveals that the ground state is the most homogeneous (liquid-like) for $U \approx U_F$, consistently with the maximum in the phase sensitivity.

An analysis of different system sizes shows that these features persist in the thermodynamic limit. Even though the system stays an insulator for all values of the interaction strength, the size dependence of the phase sensitivity allows to extract a many-body localization length, which is slightly enhanced by the interactions and maximum at $U_F$.

While the interaction-induced enhancement of the phase sensitivity is a rather small effect for the ensemble average, it can reach several orders of magnitude in individual samples, at sample-dependent values $U_c$. At these values of the interaction strength, abrupt reorganizations of the many-body ground state structure occur. The transition from the Anderson insulator to the Mott insulator, upon increasing the strength of the repulsive interaction, is typically made in two steps. In a finite size system, the first change of the ground state structure at $U_c$ is followed, at much larger interaction values $U_m \propto W$, by the installation of the Mott insulator. The interaction strength $U_m$ diverges in the thermodynamic limit, reflecting the fact that the perfect order of the Mott insulator is destroyed by an arbitrarily small amount of disorder in an infinite size system. We have found that the reorganizations of the ground state structure correspond to avoided level crossings between the many body ground state and the first excited

state, as a function of the interaction strength. We have used simple toy-models to clarify the relationship between avoided crossings, charge reorganizations, and peaks in the phase sensitivity.

The two limits of weak and strong interaction can be understood using perturbative schemes. Recently published Hartree-Fock results [61] exhibit some qualitative similarities with our quasi-exact results. However, the average phase sensitivity is strongly underestimated by Hartree-Fock at strong interaction values. A direct comparison of the phase sensitivity for individual samples [62] shows that Hartree-Fock is rather accurate for weak interaction values up to the first charge reorganization ($U < U_c$), but fails for stronger interactions when the ground state is very different from the non-interacting ground state. In the regime of very strong interaction, a perturbative development starting from the Mott insulator can describe quantitatively the phase sensitivity for $U > U_m$.

In contrast, the intermediate regime $U_F < U < U_W$ where both, interaction and disorder play an important role, is intrinsically non-perturbative and more difficult to analyze. The interplay of interactions and disorder leads to strong electronic correlations in the intermediate regime, resulting in a behavior qualitatively different from the two limiting situations.

In the limit of strong disorder, we were able to provide a rough estimate of the probability of observing a charge reorganization in a given sample, as a function of the particle density and the system size. This shows that for strong disorder, half filling is the optimal condition to obtain interaction-induced charge reorganizations. At lower electronic densities, the probability in finite-size samples is reduced with respect to this optimal situation. However, when the disorder strength is reduced simultaneously, such that the one-particle localization length is of the order of the inter-particle distance, the reduction of the probability is less important. We expect that the use of a long-range interaction could also favor the occurrence of charge reorganizations.

We recall the fact that the delocalization effect of repulsive interactions has been predicted in models other than that of our work: Disordered Hubbard models in 1D [23] and in 2D [63], systems with strong binary disorder [44], rings coupled to a side stub [57], and interacting bosons in a disordered chain [64].

As discussed in the introduction, the understanding of the metal-insulator transition in disordered two-dimensional systems has been one of our motivations for this study. Even if our model is much simpler than the realistic problem of interest, it contains non-trivial features that may be useful to understand the transition, like the concept of charge reorganization discussed above. The intermediate regime that we find between the limits of weak and strong interactions can be considered as a precursor of the correlated phase found in numerical studies [13] of two dimensional disordered clusters (with long-range Coulomb interaction) when the Wigner molecule is about to be formed. Consistently with our results, the use of the Kubo-Greenwood formula and an exact diagonalization in a truncated basis of Hartree-Fock states [65] yields an average conductance which is slightly increased by a small repulsive interaction for spinless electrons in strongly disordered 2D systems.

Recent experimental measurements of the local compressibility in the localized phase of a two-dimensional system [66] yielded important spatial inhomogeneities and very large fluctuations as a function of the carrier density, while the metallic phase appeared as spatially homogeneous and less fluctuating. The strong fluctuations of the localized phase can be interpreted as charge reorganizations, very much in line with the interpretation of peaks in the phase sensitivity that we have thoroughly discussed in our work.

Since the existing numerical work in two dimensions relies on some drastic approximations or is restricted to small systems, it could be useful to extend our numerical techniques beyond the one-dimensional case. In addition, the electron spin has been shown experimentally to play a major role in the metal-insulator transition [9,67], and it should be interesting to relax the condition of spinless fermions in order to approach the realistic case.

# References

1. N.W. Ashcroft, N.D. Mermin, *Solid State Physics* (Saunders College, Philadelphia, 1976).
2. L.P. Lévy, G. Dolan, J. Dunsmuir, H. Bouchiat, Phys. Rev. Lett. **64**, 2074 (1990).
3. V. Chandrasekhar, R.A. Webb, M.J. Brady, M.B. Ketchen, W.J. Gallagher, A. Kleinsasser, Phys. Rev. Lett. **67**, 3578 (1991).
4. P. Mohanty, E.M.Q. Jariwala, M.B. Ketchen, R.A. Webb, in *Quantum Coherence and Decoherence*, edited by K. Fujikawa, Y.A. Ono (Elsevier, 1996).
5. A. Schmid, Phys. Rev. Lett. **66**, 80 (1991); F. von Oppen, E.K. Riedel, *ibid.*, p. 84; B.L. Altshuler, Y. Gefen, Y. Imry, *ibid.*, p. 88.
6. U. Eckern, Z. Phys. B **42**, 389 (1991).
7. U. Eckern, P. Schwab, Adv. Phys. **44**, 387 (1995).
8. S.V. Kravchenko *et al.*, Phys. Rev. B **50**, 8039 (1994); *ibid.* **51**, 7038 (1995).
9. A.R. Hamilton *et al.*, Phys. Rev. Lett. **82**, 1542 (1999).
10. J. Lam *et al.*, Phys. Rev. B **56**, R12741 (1997); P.T. Coleridge, *ibid.*, R12764.
11. E. Abrahams, P.W. Anderson, D.C. Licciardello, T.V. Ramakrishman, Phys. Rev. Lett. **42**, 673 (1979).
12. E. Abrahams, S.V. Kravchenko, M.P. Sarachik, Rev. Mod. Phys. (in press), `cond-mat/0006055`.
13. G. Benenti, X. Waintal, J.-L. Pichard, Phys. Rev. Lett. **83**, 1826 (1999).
14. B. Spivak, `cond-mat/0005328`.

15. P. Mohanty, E.M.Q. Jariwala, R.A. Webb, Phys. Rev. Lett. **78**, 3366 (1997).
16. V.E. Kravtsov, B.L. Altshuler, Phys. Rev. Lett. **84**, 3394 (2000).
17. P. Mohanty, Ann. Phys. (Leipzig) **8**, 549 (1999); Physica B **280**, 446 (2000), `cond-mat/9912263`.
18. P. Schwab, Eur. Phys. J. B **18**, 189 (2000), `cond-mat/0005525`.
19. A. Luther, I. Peschel, Phys. Rev. B **9**, 2911 (1973).
20. T. Giamarchi, H. Schulz, Phys. Rev. B **37**, 325 (1988).
21. R. Shankar, Int. J. Mod. Phys. B **4**, 2371 (1990).
22. B. Sutherland, B.S. Shastry, Phys. Rev. Lett. **65**, 1833 (1990).
23. T. Giamarchi, B.S. Shastry, Phys. Rev. B **51**, 10915 (1995).
24. A. Müller-Groeling, H.A. Weidenmüller, C.H. Lewenkopf, Europhys. Lett. **22**, 193 (1993); A. Müller-Groeling, H.A. Weidenmüller, Phys. Rev. B **49**, 4752 (1994).
25. H. Pang, S. Liang, J.F. Annett, Phys. Rev. Lett. **71**, 4377 (1993).
26. M. Abraham, R. Berkovits, Phys. Rev. Lett. **70**, 1509 (1993).
27. G. Bouzerar, D. Poilblanc, G. Montambaux, Phys. Rev. B **49**, 8258 (1994).
28. H. Kato, D. Yoshioka, Phys. Rev. B **50**, 4943 (1994).
29. E.V. Tsiper, A.L. Efros, J. Phys. Cond. Matt. **9**, L561 (1997); Phys. Rev. B **57**, 6949 (1998).
30. P. Schmitteckert, T. Schulze, C. Schuster, P. Schwab, U. Eckern, Phys. Rev. Lett. **80**, 560 (1998).
31. G.S Jeon, S. Wu, H.W. Lee, M.Y. Choi, Phys. Rev. B **59**, 3033 (1999).
32. G. Chiappe, J.A. Vergés, E. Louis, Solid State Commun. **99**, 717 (1996).
33. H.F. Cheung, Y. Gefen, E.K. Riedel, W.H. Shih, Phys. Rev. B **37**, 6050 (1988).
34. T. Okabe, J. Phys. Soc. Jpn **67**, 7292 (1998).
35. W. Kohn, Phys. Rev. **133**, A171 (1964).
36. D. Scalapino, S.R. White, S. Zhang, Phys. Rev. B **47**, 7995 (1995).
37. A.J. Leggett, in *Granular Nanoelectronics*, edited by D.K. Ferry, J.R. Barker, C. Jacobini, NATO ASI Ser. B **251** (Plenum, New York, 1991).
38. D. Loss, Phys. Rev. Lett. **69**, 343 (1992).
39. C.A. Stafford, A.J. Millis, B.S. Shastry, Phys. Rev. B **43**, 13660 (1991).
40. R.M. Fye, M.J. Martins, D.J. Scalapino, J. Wagner, W. Hanke, Phys. Rev. B **44**, 6909 (1991).
41. P. Schmitteckert, R.A. Jalabert, D. Weinmann, J.-L. Pichard, Phys. Rev. Lett. **81**, 2308 (1998).
42. D. Weinmann, J.-L. Pichard, P. Schmitteckert, R.A. Jalabert, in *Quantum Physics at Mesoscopic Scale, Proceedings of the XXXIVth Rencontres de Moriond*, edited by C. Glatti, M. Sanquer, J. Trân Thanh Vân (EDP Sciences, Les Ulis, 2000), p. 69, `cond-mat/9905017`.
43. R.A. Jalabert, D. Weinmann, J.-L. Pichard, Physica E (in press).
44. M. Ulmke, V. Janiš, D. Vollhardt, Phys. Rev. B **51**, 10411 (1995).
45. D.L. Shepelyansky, Phys. Rev. Lett. **73**, 2607 (1994).
46. X. Waintal, D. Weinmann, J.-L. Pichard, Eur. Phys. J. B **7**, 451 (1999).
47. S. De Toro Arias, X. Waintal, J.-L. Pichard, Eur. Phys. J. B **10**, 149 (1999).
48. A. Wobst, D. Weinmann, Eur. Phys. J. B **10**, 159 (1999).
49. S.R. White, Phys. Rev. B **48**, 10345 (1993).
50. *Density-Matrix Renormalization – A New Numerical Method in Physics*, edited by I. Peschel, X. Wang, M. Kaulke, K. Hallberg (Springer, Berlin, 1999).
51. X. Waintal, G. Benenti, J.-L. Pichard, Europhys. Lett. **49**, 466 (2000).
52. G. Benenti, X. Waintal, J.-L. Pichard, Europhys. Lett. **51**, 89 (2000).
53. A.F. Andreev, I.M. Lifshitz, Sov. Phys. JETP, **29**, 1107 (1969).
54. Y. Imry, S. Ma, Phys. Rev. Lett. **35**, 1399 (1975).
55. C.W.J. Beenakker, Phys. Rev. B **44** 1646 (1991).
56. G. Benenti, X. Waintal, J.-L. Pichard, D.L. Shepelyansky, Eur. Phys. J. B **17**, 515 (2000).
57. P. Cedraschi, M. Büttiker, J. Phys. C **10**, 3985 (1998).
58. H. Bouchiat, G. Montambaux, J. Phys. France **50**, 2695 (1989).
59. C.A. Stafford, A.J. Millis, Phys. Rev. B **48**, 1409 (1993).
60. F. Selva, D. Weinmann, Eur. Phys. J. B **18**, 137 (2000), `cond-mat/0003202`.
61. A. Kambili, C.J. Lambert, J.H. Jefferson, Phys. Rev. B **60**, 7684 (1999).
62. F. Piechon, G. Montambaux, private communication.
63. R. Kotlyar, S. Das Sarma, Phys. Rev. Lett. (in press), `cond-mat/0002304`.
64. R.T. Scalettar, G.G. Batrouni, G.T. Zimanyi, Phys. Rev. Lett. **66**, 3144 (1991).
65. T. Vojta, F. Epperlein, M. Schreiber, Phys. Rev. Lett. **81**, 4212 (1998).
66. S. Ilani, A. Yacoby, D. Mahalu, H. Shtrikman, Phys. Rev. Lett. **84**, 3133 (2000).
67. D. Simonian, S.V. Kravchenko, M.P. Sarachik, V.M. Pudalov, Phys. Rev. Lett. **79**, 2304 (1997).